

## PARAMETERS IDENTIFICATION OF A POWER PLANT MODEL FOR THE SIMULATION OF ISLANDING TRANSIENTS

Alberto BORGHETTI<sup>1</sup>, Mauro BOSETTI<sup>2</sup>, Carlo ALBERTO NUCCI<sup>3</sup>, Mario PAOLONE<sup>4</sup>

*The paper presents a procedure for parameter identification along with its application to the model of a combined cycle power plant that includes the surrounding electrical network, built for the analysis of islanding maneuvers transients. The paper illustrates both the power system computer model, implemented within the EMTP-RV simulation environment, and the developed identification procedure based on the interface between the developed model and Matlab. The parameter identification procedure is applied to experimental transient recordings that make reference to a similar power plant.*

**Keywords:** power plant, parameter identification, islanding, electromechanical transients

### 1. Introduction

The complexity of power plants operation, of their interaction with the electrical network, as well as the need of implementing coordinated control systems to cope with specific operational requirements, call for the development/use of advanced and accurate simulation tools. This may represent the adequate complement or substitute the practice of repetitive prototyping and expensive tests on real systems.

Within this context, the parameter identification of power plant dynamic models represents one of the main issues for proper simulation of the transients occurring during critical operation conditions [1-3]<sup>\*)</sup>.

This paper deals with a parameter-identification procedure conceived for the development of a computer simulator aimed at reproducing the islanding and black-startup energization transients of a power system consisting of a combined

<sup>1</sup> Prof., Department of Electrical Engineering, University of Bologna, Italy

<sup>2</sup> Prof., Department of Electrical Engineering, University of Bologna, Italy

<sup>3</sup> Prof., Department of Electrical Engineering, University of Bologna, Italy

<sup>4</sup> Prof., Department of Electrical Engineering, University of Bologna, Italy

<sup>\*)</sup> The contents of the paper are based on a previous work presented at by the Authors at the 9th International Conference on Modeling and Simulation of Electric Machines, Converters and Systems (Electrimacs 2008), June 8-11, 2008, Québec city, Canada.

cycle power plant (CCPP), the local distribution network and relevant loads, (see Fig. 1).

In particular, the computer simulator refers to a 80 MW power plant composed by two aero-derivative gas turbine (GT) units and a steam turbine unit (ST) in combined cycle. The simulator represents the dynamic behavior of the GTs, the heat recovery steam generator (HRSG), the ST and their control systems [4-8]. Concerning the electrical apparatus, it includes the model of the synchronous generators along with their excitors, automatic voltage regulators (AVRs) [9-10], as well as the representation of the local electrical network (step-up unit transformers, cable link between power plant substation and distribution substation and loads) connected to the external transmission network.

All the models are implemented in the EMTP-RV simulation environment ([11-13]) and are aimed at representing both transients following energization process, typically after a blackout condition, and transients due to islanding maneuvers that disconnect the CCPP and the local network from the external transmission network.

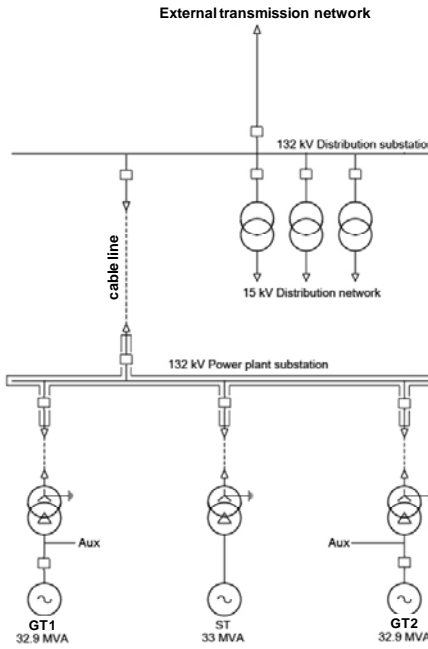


Fig.1. Scheme of the considered CCPP and the surrounding electrical network

The applied parameter identification procedure is based on an interface between the EMTP-RV and Matlab that has been developed to implement a non-linear data fitting algorithm. The parameter identification procedure makes use of available test recordings.

The structure of the paper is the following. Section II provides an overview of the models implemented in the EMTP-RV computer simulator. Section III describes the earlier mentioned interface between EMTP-RV and Matlab. Section IV and Section V present the application of the developed procedure for the identification of the key model parameters by using experimental transients recorded during load rejection maneuvers. In particular, Section IV is devoted to the identification of the GT AVR parameters, whilst Section V focuses on the identification of the parameters of the GT dynamic model and its governor. Section VI is devoted to the conclusions.

## 2. Overview of the computer simulator

As is illustrated in Fig.1, the synchronous generators of the three units are connected to a 132 kV power plant substation through 15/132 kV step-up transformers. The power plant substation is assumed to be linked, by means of a cable line, to a distribution substation that feeds the local loads and provides the connection with the external transmission network.

For the cable line, two models have been implemented: the frequency dependent model [14] and the exact  $\Pi$ -model, both obtained by making reference to the manufacturer data of the 132 kV three-phase cable. The two different models are adopted for the simulation of electromagnetic transients and electromechanical ones respectively.

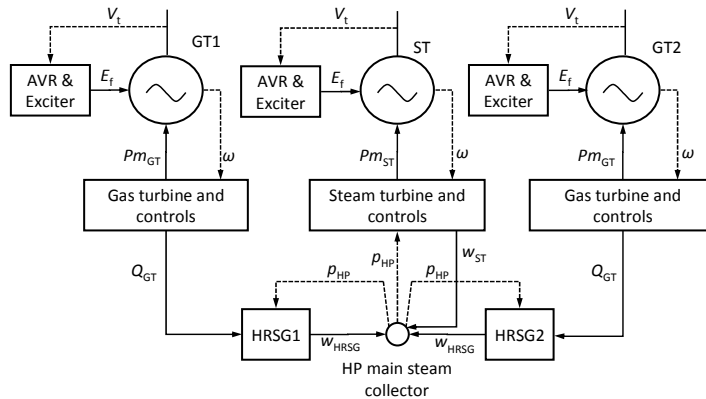


Fig. 2. Block diagram of the simulated power plant and relevant controls

Fig. 2 shows the main parts of the power plant model, namely the synchronous machines (for which saturation curves have been taken into account), the excitation systems with the relevant AVR, the prime movers (GTs and ST), the HRSGs and the high pressure (HP) main steam collector. The same figure also shows the main variables connecting the various parts of the power plant model:

|            |  |
|------------|--|
| $V_t$      | terminal voltage of the synchronous generators |
| $E_f$      | field voltage                                  |
| $\omega$   | angular speed of the generators rotors         |
| $P_{mGT}$  | mechanical output power of a GT                |
| $P_{mST}$  | mechanical output power of the ST              |
| $Q_{GT}$   | thermal power provided by the GT exhaust gas   |
| $w_{HRSG}$ | output steam mass flow rate of a HRSG          |
| $w_{ST}$   | inlet steam mass flow to the ST                |
| $p_{HP}$   | pressure in the HP main steam collector.       |

The initial states of the GTs models, the excitation systems and the AVR models are defined by the results of the initial network power flow calculation. The states of the HRSGs and the states of the ST model are initialized from the initial values of  $Q_{GT1}$ ,  $Q_{GT2}$  and those of  $w_{HRSG1}$ ,  $w_{HRSG2}$  respectively, assuming pressure  $p_{HP}$  be equal to the rated value and that the by-pass valves be closed.

Each of the three synchronous generators has two inputs: excitation voltage  $E_f$  and mechanical power  $P_m$ .

The excitation voltages are provided by the AVR and brushless exciter models of the GT units and ST unit. The model of GT AVR and exciter corresponds to the AC8B Type of the IEEE Std. 421. [9]. The GT AVR parameter values are identified from available load rejection transient record, as described in Section IV. The ST AVR is based on a simple PI regulator with a lead-lag compensator.

The mechanical power values are provided by the models of the GTs ( $P_{mGT}$ ) and the one of the ST ( $P_{mST}$ ).

Table 1

Values of the synchronous machines electrical parameters

|    | $x_d$ | $x'_d$ | $x''_d$ | $x_q$ | $x'_q$ | $T_d$ | $T''_d$ | $T_q$ | $x_0$ | $x_l$ |
|----|-------|--------|---------|-------|--------|-------|---------|-------|-------|-------|
| GT | 2.13  | 0.29   | 0.18    | 1.09  | 0.43   | 1.09  | 0.04    | 0.04  | 0.13  | 0.13  |
| ST | 2.2   | 0.29   | 0.2     | 1.11  | 0.4    | 1.3   | 0.08    | 0.075 | 0.07  | 0.15  |

The model adopted for the two GTs is based on a transfer function that represents the dynamic link between fuel flow rate and output mechanical power and includes the fuel metering valve (FMV) dynamic and a speed governor. Section V is devoted to the parameter identification of the GT model and of its speed governor, together with the parameter identification of a two-mass model of the GT train drive.

The HRSG model is adapted from the one proposed in [5], relevant to the HP section with a bypass control valve at the HRSG output. The model is based on the following main assumptions: fast feed water adjustments, negligible effects of temperature control and water flows to the attemperators, constant enthalpy value of the steam at the ST inlet.

As shown in Fig. 2 and Fig. 2, the inputs of the HRSG model are QGT and pHp. QGT is assumed to be a non-linear function of the gas turbine output power PmGT [4]. Concerning pHp, it is calculated from the difference between the steam mass flow rate at the HRSGs outputs (wHRSG) and the steam turbine inlet mass flow rate (wST) through a transfer function that takes into account the time constant associated with the steam storage capacity into the collector volume.

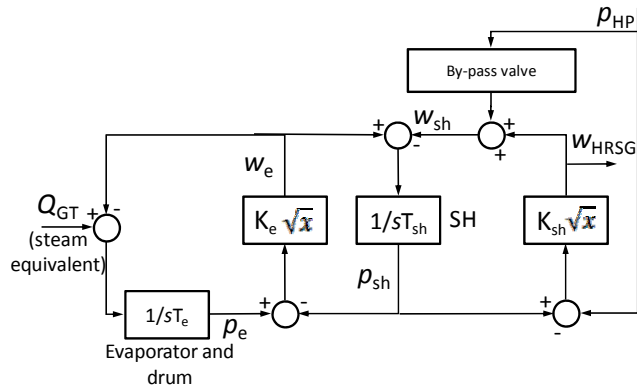


Fig. 3. Model of the HRSG

Fig. 3 illustrates the structure of the implemented HP section HRSG model, which takes into account the evaporator time constant  $T_e$  for the calculation of the pressure  $p_e$  in the drum according to the energy balance equation, a time constant  $T_{sh}$  relevant to the superheaters (SH) storage capacity. The steam flow rates between drum and SH and between SH and the collector are determined from the pressure drop relationship with flow rate being proportional to square root of pressure drop.

The model of the steam turbine, shown in Fig. 4, represents the time delay associated with the steam store in the inlet chest, the main valve dynamic implements three control operation modes: i) no-load speed control, ii) control to keep a constant value of upstream pressure  $p_{HP}$ , iii) power and speed regulation. The no-load speed control mode is used at the startup and synchronizing phases, whilst in normal conditions the two modes are the pressure control or power-speed regulation.

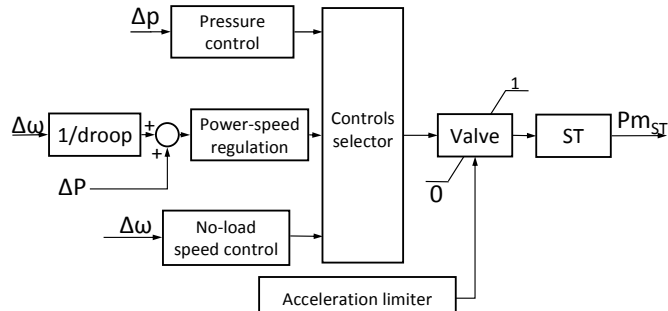


Fig. 4. Model of the ST and its controls

### 3. Identification procedure

The modern conception of simulation tools, such as EMTP-RV, allows to interface the simulation environment with external software, as, for instance, those used for signal processing calculations and parameter identification. EMTP RV is used indeed for such a purpose in order to carry out multiple simulations and to retrieve the data of the quantities of interest of the resulting transients. These data are compared with the available experimental ones. An optimization problem is then solved to obtain the most adequate values of the model parameters, as described in what follows.

Being  $\mathbf{p} = [p_1, p_2, \dots, p_i, \dots, p_n]$  the set of  $n$  model parameters to be identified,  $\mathbf{p}_0$  a vector of the initial guess values,  $\mathbf{s}(\mathbf{p})$  the vector of  $N$  samples of the calculated transient by using parameter vector  $\mathbf{p}$ , the optimization problem tries to find parameter vector  $\mathbf{p}^*$  that minimizes the norm of the difference between the calculated transient and the available experimental data  $\mathbf{s}_e$ :

$$\mathbf{p}^* = \arg \min_{\mathbf{p}} \frac{1}{2} \|F(\mathbf{p})\|_2^2, \quad (1)$$

where

$$F(\mathbf{p}) = \begin{bmatrix} s_{e,1} - s_1(\mathbf{p}) \\ \dots \\ s_{e,i} - s_i(\mathbf{p}) \\ \dots \\ s_{e,N} - s_N(\mathbf{p}) \end{bmatrix}, \quad (2)$$

The optimization problem is implemented in a Matlab script and solved by using the `lsqnonlin` function of the Optimization Toolbox. The interface between Matlab and EMTP-RV environment is provided by specific Matlab scripts that allow the communication between the two programs, as illustrated in Fig. 5.

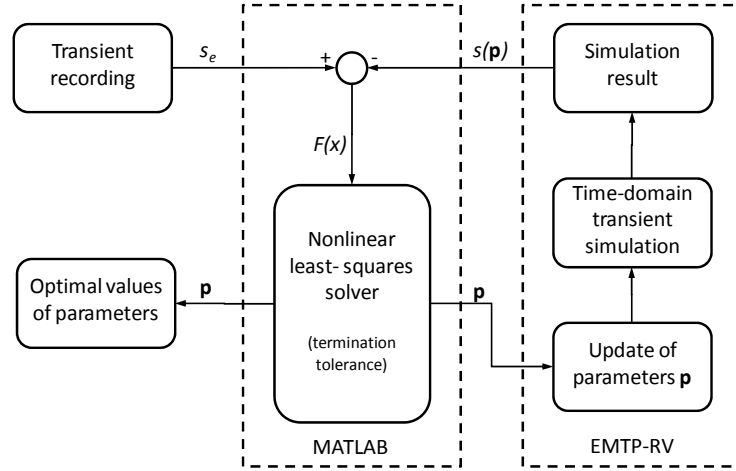


Fig. 5. Scheme of the identification procedure

A Matlab script allows the access to the EMTP-RV input file (.net file) in order to read the initial values and write the updated values of the parameters. Another Matlab script is able to retrieve the analyzed signal from the EMTP-RV output file (.mda file) that contains the simulation results. The scripts are able to retrieve the observed signal waveform from the results database and make it available within the Matlab workspace and also subsequently execute the EMTP-RV simulations.

#### 4. Identification of GT automatic voltage regulator parameters

##### 4.1 Description of the adopted model

The excitors of the GT units are of brushless type. This kind of excitors supply the field circuit of the synchronous generator by a DC voltage produced using the combined action of an AC generator and a non-controlled diode rectifier. The main data of the exciter are reported in Table II.

Table 2

Data of the GT exciter

|                           | Stator | Rotor |
|---------------------------|--------|-------|
| No load voltage (V)       | 17     | 27    |
| No load current (A)       | 2.8    | 283   |
| Exciter rated current (A) | 50     | 80    |
| Rated current (A)         | 8.2    | 841   |
| Ceiling voltage (V)       | 98     | 153   |
| Ceiling current (A)       | 16.1   | 1618  |
| Exciter response (1/s)    | 2.24   |       |

As already mentioned, the model adopted for the exciter corresponds to Type AC8B of IEEE Std. 421 [9], illustrated in Fig. 6. The AVR is a PID control

with independent values of the proportional ( $K_P$ ), integral ( $K_I$ ), and derivative ( $K_{DIFF}$ ) gains and derivative time constant  $T_d$ . The behavior of brushless excitors depends on the generator loading condition and requires also the field current as input. This kind of excitors does not allow negative values for the field voltage and current. As illustrated by Fig. 6 the exciter voltage  $V_E$  is corrected by a feedback ring that takes into account the sum of three contributions: (i) the product between  $V_E$  and the saturation function  $S_E(V_E)$ , (ii) the product between  $V_E$  and exciter constant  $K_E$  and (iii) the product between demagnetizing factor  $K_D$  and field current  $I_f$ .

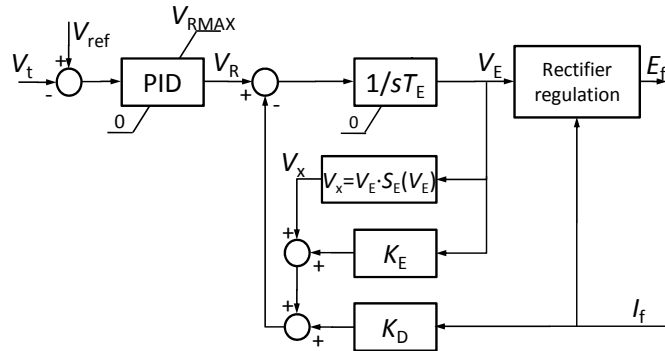


Fig. 6. Model of GT AVR and excitation system

The characteristic of the exciter saturation function  $S_E$  included in the model is shown in Fig. 7.

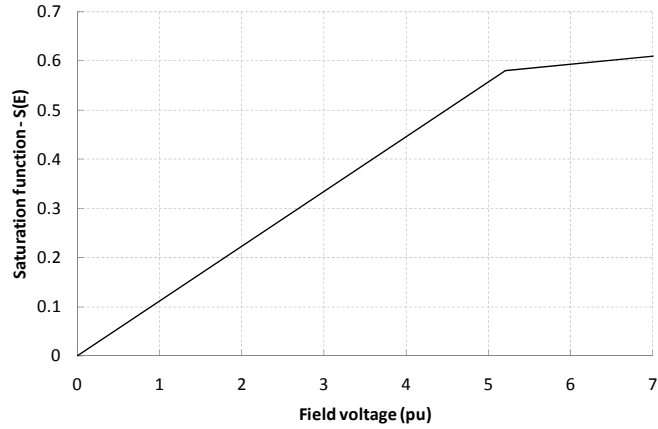


Fig. 7. Exciter saturation function

The output field voltage  $E_f$  is calculated taking into account also the reduction due to the commutation reactance of the rectifier, by means the rectifier

regulation block. As explained in [9], the impedance of the AC source supplying the AC side of rectifiers is characterized by predominantly inductive impedance. The impedance causes a strongly non linear decrease of the rectifier voltage output. This effect depends on the value of the current supplied by the rectifier and is represented by means a rectifier loading factor  $K_c$  proportional to commutating reactance and the rectifier regulation characteristic.

The values of the main parameters adopted for the exciter model are reported in Table III.

Table 3

**– Values of the main parameters of the GT exciter model**

|                        |                   |                          |
|------------------------|-------------------|--------------------------|
| $V_{RMAX} = 11.9$      | $K_C = 0.29$      | $K_D = 1.03$             |
| $K_E = 1.0$            | $T_E = 0.31$      | $E_1 = 5.2 \text{ p.u.}$ |
| $E_2 = 7 \text{ p.u.}$ | $S_E(E_1) = 0.58$ | $S_E(E_2) = 0.61$        |

#### 4.2. Identification results

The AVR parameter identification is based on the recorded transient of the terminal voltage  $V_t$  of a GT unit after a load rejection at rated output. The set of parameters selected for the optimal identification is  $\mathbf{p} = [K_p, K_I, K_{DIFF}, T_d]$ .

Fig. 8 shows the comparison between the experimental voltage transient and the simulation results using the implemented model. Table IV shows the initial guess values and the identified values of the AVR parameters, together with the allowed range of variations, and the example values reported in [9].

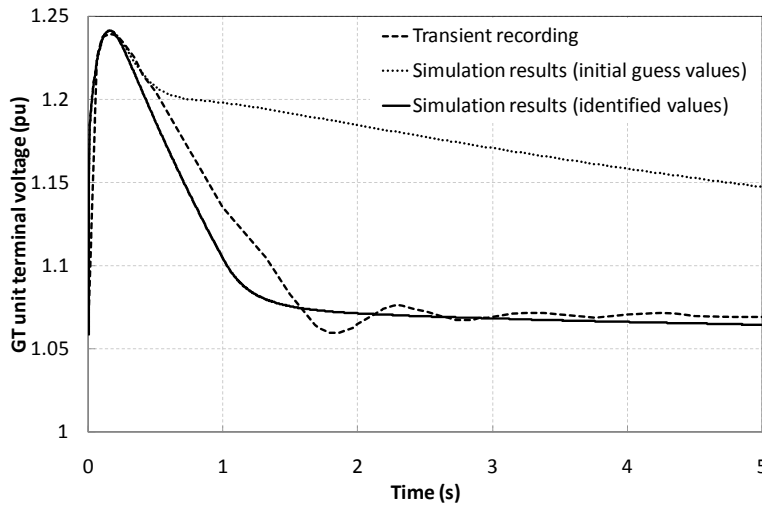


Fig. 8. Comparison between a full load rejection voltage transient at the GT unit terminals and the corresponding transients obtained by using the implemented model

*Table 4*

**Initial and identified AVR parameters, together with the allowed range of variations and the example values reported in [9]**

| Parameter  | Initial guess values | Std. IEEE example values | Range | Identified values |
|------------|----------------------|--------------------------|-------|-------------------|
| $K_p$      | 35                   | 80                       | 7-280 | 132.8             |
| $K_I$      | 5                    | 5                        | 1-100 | 35.05             |
| $K_{DIFF}$ | 6                    | 10                       | 1-80  | 25.58             |
| $T_d$      | 0.1                  | 0.1                      | -     | 0.012             |

## 5. Identification of the parameters of the GT dynamic model and its governor

### 5.1. Description of the adopted model

The considered GT is an aeroderivative industrial RB211 package, characterized by a rated output to the electrical generator equal to 33 MW at 4850 rpm speed and by 94 kg/s exhaust mass flow at 503 °C.

The adopted model is illustrated in Fig. 9. As already mentioned the GT dynamics is represented by 4 poles-4 zeros transfer function that represent the dynamic link between fuel flow rate and output mechanical power

$$GT(s) = K_{\text{GT}} \frac{(\tau_{z1}s+1)}{(\tau_{p1}s+1)} \cdot \frac{(\tau_{z2}s+1)}{(\tau_{p2}s+1)} \cdot \frac{(\tau_{z31}s^2 + \tau_{z32}s + 1)}{(\tau_{p31}s^2 + \tau_{p32}s + 1)}, \quad (3)$$

A feedback algebraic look-up table block determines the required correction at partial loads.

The FMV dynamic is represented by a first order transfer function with time constant TFMV equal to 0.1 s.

The droop of the speed governor is assumed equal to 5%. The model includes also an acceleration limiter.

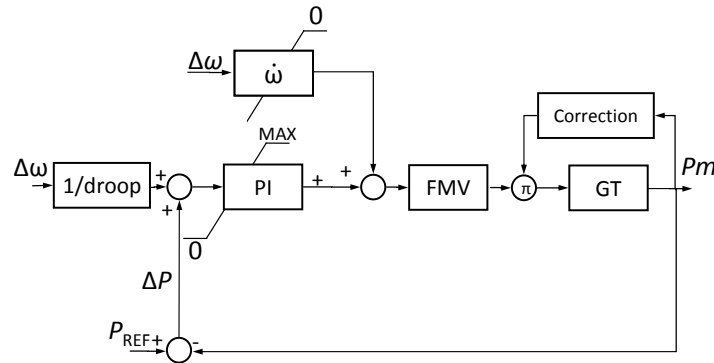


Fig. 9. Model of the GT and its speed governor

The GT is connected to the rotor of the synchronous machine by means of a mechanical gearbox with transmission ratio equal to 1500/4850. Fig. 10 illustrates the adopted two-mass model of the GT drive trains. Mass 1 represents the inertia of the low-speed GT shaft and the gearbox, whilst mass 2 represents the generator rotor. The same figure shows the model parameters, namely

|                |  |
|----------------|--|
| $H_1, H_2$     | inertia constant of mass 1 and 2, respectively;  |
| $HSP$          | spring constant pertaining to the elastic connection between the two masses;                   |
| $DSR_1, DSR_2$ | speed deviation self-damping coefficient for each mass;  |
| $DSD_1$        | absolute speed self-damping coefficient of mass 1, subject to the GT mechanical torque $T_m$ . |

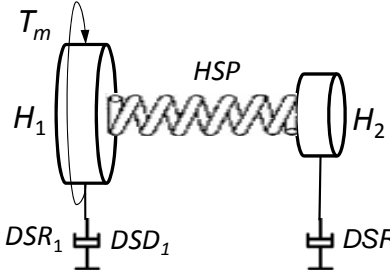


Fig. 10. Scheme of the GT drive train two-mass model

The  $H_2$  value is assumed equal to 1.285 s. The  $DSD_1$  value is assumed equal to 48 Nms/rad, in order to take into account the power losses associated with the gearbox (1.2 MW at synchronous speed of 1500 rpm).

### 5.2 Identification results

The identification procedure is applied in two steps. In the first step, the identification is based on the GT speed transient recorded during a load rejection from 18 MW to no-load full-speed condition. In this step, the parameters of the GT transfer function and the parameters of the GT drive train are identified assuming a closing step input to the FMV block.

Fig. 11 shows the comparison between the experimental GT angular speed transient and the corresponding simulation results using the implemented model. Table V shows the initial guess values and the identified parameter values of the GT transfer function and the drive train model.

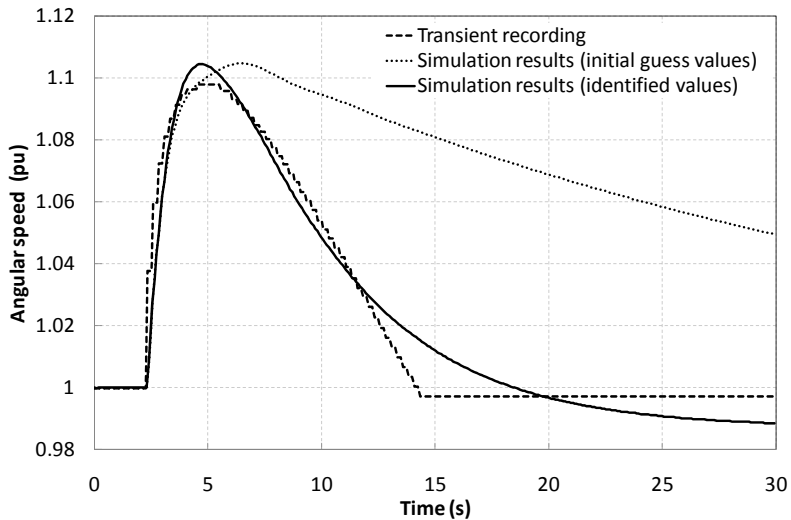


Fig. 11. Comparison between the GT angular speed transient recorded during a 18 MW load rejection and the corresponding transients obtained by using the implemented model

Table 5

Initial and identified parameters of the GT model

| Parameter         | Initial guess value | Optimized values   |
|-------------------|---------------------|--------------------|
| $\tau_{22}$ (s)   | 3.13                | 0.06               |
| $\tau_{p2}$ (s)   | 30.03               | 5.15               |
| $\tau_{z31}$ (s)  | 0.032               | 0.24               |
| $\tau_{z32}$ (s)  | 0.31                | 0.16               |
| $\tau_{b31}$ (s)  | 0.38                | 0.3                |
| $\tau_{b32}$ (s)  | 1.08                | 1.08               |
| $H_1$ (s)         | 0.73                | 0.89               |
| $DSR_1$ (Nms/rad) | $5 \cdot 10^3$      | $3.67 \cdot 10^3$  |
| $HSP$ (Nm/rad)    | $4 \cdot 10^6$      | $7.858 \cdot 10^6$ |
| $DSR_2$ (Nms/rad) | 0                   | 0                  |

In the second identification step relevant to the proportional ( $K_{govP}$ ) and integral ( $K_{govI}$ ) speed governor parameters, we use, as reference, the Pm transients provided by the Rolls-Royce Aeroengine Performance Program (RRAP) for small perturbations of the  $\Delta\omega$  speed governor input at 20 MW initial power output. In particular the  $\Delta\omega$  varies as a sinusoid function, with amplitude equal to 5 rpm and frequency equal to 0.2 Hz, followed, after 25 s, by a 1.73 rpm positive step and, after 85 s, a 3.46 rpm negative step.

Fig. 12 shows the comparison between the Pm transients obtained by the detailed RRAP and the implemented model. Table VI shows the initial guess values and the identified parameter values of the GT speed governor model.

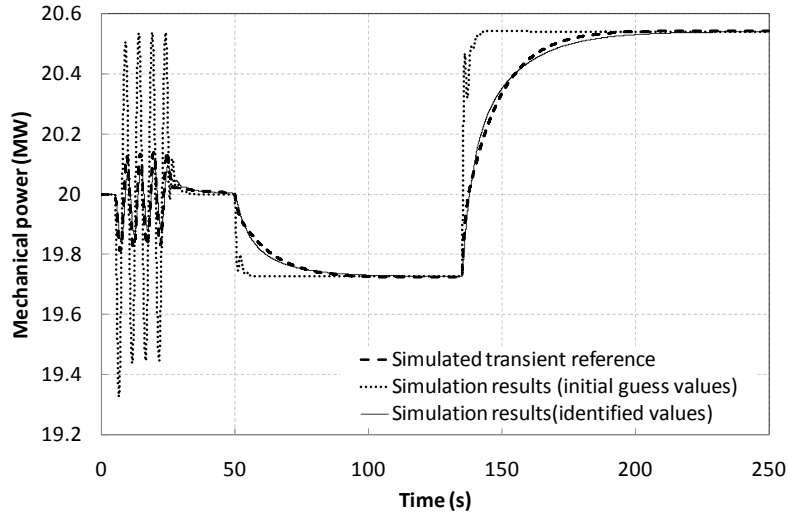


Fig. 12. Comparison between the GT Pm transient simulated with a detailed model (reference) and those obtained by the implemented model, for small speed perturbations

Table 6

**Initial and identified parameters of the GT speed governor model**

| Parameter   | Initial guess value | Identified values |
|-------------|---------------------|-------------------|
| $K_{gov_p}$ | 7.5                 | 2.1               |
| $K_{gov_I}$ | 0.25                | 0.23              |

## 6. Conclusions

The paper has proposed an identification procedure based on the coordinated use of a run-control interface between EMTP-RV and Matlab. The structure of the interface makes available the optimization tools of Matlab that have been used within the identification procedure.

The developed interface has been effectively applied for the parameter identification of a CCPP model aimed at simulating transients following energization process and transients due to islanding maneuvers.

The identified model appears a useful tool for the definition of both operational strategies and specific control systems in order to improve the probability of success of islanding maneuvers taking into account the various CCPP initial operating conditions.

## R E F E R E N C E S

- [1]. *J. L. Sancha, M. L. Llorens, J. M. Moreno, B. Meyer, J. F. Vernotte, W. W. Price, J. J. Sanchez-Gasca*, “Application of long term simulation programs for analysis of system islanding,” *IEEE Transactions on Power Systems*, **vol. 12**, no. 1, pp. 189–197, Feb. 1997
- [2]. CIGRE TF38.02.14, “Analysis and modeling needs of power systems under major frequency disturbances,” Rep., CIGRE Brochure no. 148, 1999
- [3]. *A. Borghetti, G. Migliavacca, C.A. Nucci, S. Spelta*, “Black-start-up simulation of a repowered thermoelectric unit”, *Control Engineering Practice*, **Vol. 9**, pp. 791–803, 2001.
- [4]. Cigre Task Force C4.02.25, Modeling of Gas Turbines and Steam Turbines in Combined Cycle Power Plants, 2003
- [5]. *K. Kunitomi, A. Kurita, Y. Tada, S. Ihara, W.W. Price, L.M. Richardson, G. Smith*, “Modeling Combined-Cycle Power Plant for Simulation of Frequency Excursions”, *IEEE Transactions on Power Systems*, **Vol. 18**, No. 2, pp. 724-729, May 2003
- [6]. *S. Kiat Yee, J.V. Milanovic', F.M. Hughes*, “Overview and Comparative Analysis of Gas Turbine Models for System Stability Studies”, *IEEE Transactions on Power Systems*, **Vol. 23**, No. 1, pp. 108-118, Feb. 2008
- [7]. *M. E. Flynn, M. J. O'Malley*, “A drum boiler model for long term power system dynamic simulation,” *IEEE Transactions on Power Systems*, **vol. 14**, no. 1, pp. 209–217, Feb. 1999
- [8]. *A.E. Nielsen, C. W. Moll, S. Staudacher*, “Modeling and Validation of the Thermal Effects on Gas Turbine Transients”, *Transactions of the ASME*, **Vol. 127**, pp. 564-572, July 2005
- [9]. IEEE Std 421.5™-2005 - IEEE Recommended Practice for Excitation System Models for Power System Stability Studies
- [10]. *P. Kundur, P. L. Dandeno*, “Implementation of Synchronous Machine Models into Power System Stability Programs,” *IEEE Transactions on Power Apparatus and Systems*, **vol. PAS-102**, pp. 2047–2054, July 1983
- [11]. *J. Mahseredjian, S. Lefebvre, X.-D. Do*, “A new method for time-domain modelling of nonlinear circuits in large linear networks”, Proc. of 11th Power Systems Computation Conference PSCC, August 1993
- [12]. *J. Mahseredjian, S. Dennetière, L. Dubé, B. Khodabakhchian, L. Gérin-Lajoie*, “On a new approach for the simulation of transients in power systems”, *Electric Power Systems Research*, **Vol. 77**, Issue 11, September 2007, pp. 1514-1520
- [13]. *J. Mahseredjian*, “Simulation des transitoires électromagnétiques dans les réseaux électriques”, Édition ‘Les Techniques de l’Ingénieur’, Dossier n°D4130, Réseaux électriques et applications
- [14]. *J. Marti*, “Accurate Modeling of Frequency Dependent Transmission Lines In Electromagnetic Transient Simulations”, *IEEE Trans. On Power Apparatus and Systems*, **vol PAS-101**, pp 147-157, 1982.